**Supplementary Information for New journal of Chemistry**

**Controlled growth of oriented porous hexagonal ZnO nanosheets on Nitinol fiber as superior coatings of solid-phase microextraction coupled to HPLC-UV for preconcentration and determination of polycyclic aromatic hydrocarbons in water**

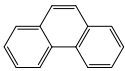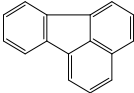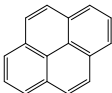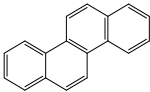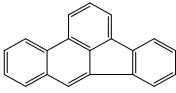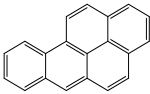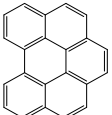Hua Zhou, [a] Haixia Liu, [a] Nian Qin, [a] Jianlan Ke, [a] Xuemei Wang, [a] Xinzhen Du [a,b*]
[a] College of Chemistry and Chemical Engineering, Northwest Normal University, Lanzhou 730070, China
[b] Key Laboratory of Eco-Functional Polymer Materials of the Ministry of Education, Lanzhou 730070, China
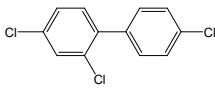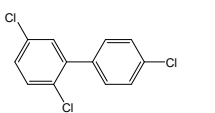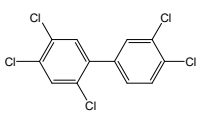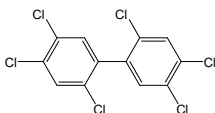
**2 Experimental**
2.1 Materials and reagents

**Table S1** The chemical structures and properties of seven PAHs.

| Compounds | Structures | Rings | Molecular formula | Relative molecular mass (g·mol$^{-1}$) | log$K_{ow}$[a] |
|---|---|---|---|---|---|
| Phenanthrene (Phe) | | 3 | $C_{14}H_{10}$ | 178.23 | 4.62 |
| Fluoranthene (Flu) | | 4 | $C_{16}H_{10}$ | 202.25 | 5.04 |
| Pyrene (Pyr) | | 4 | $C_{16}H_{10}$ | 202.25 | 5.12 |
| Chrysene (Chr) | | 4 | $C_{18}H_{12}$ | 228.29 | 5.69 |
| Benzo[b]fluoranthene (B[b]f) | | 5 | $C_{20}H_{12}$ | 252.31 | 5.86 |
| Benzo[a]pyrene (B[a]p) | | 5 | $C_{20}H_{12}$ | 252.31 | 6.16 |
| Benzo[g,h,i]perylene (B[ghi]p) | | 6 | $C_{22}H_{12}$ | 276.33 | 6.64 |
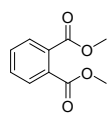
[a] log$K_{ow}$, octanol-water partition coefficients.

**Table S2** The chemical structures and properties of five PCBs.

| Compounds | Structures | Molecular formula | Relative molecular mass (g·mol⁻¹) | logK_ow^a |
|---|---|---|---|---|
| 2,4,4'-Trichlorobiphenyl (PCB 28) | | $C_{12}H_7Cl_3$ | 257.54 | 5.62 |
| 2,4',5-Trichlorobiphenyl (PCB 31) | | $C_{12}H_7Cl_3$ | 257.54 | 5.41 |
| 2,3′,4,4′,5-Pentachlorobiphenyl (PCB-118) | | $C_{12}H_5Cl_5$ | 326.43 | 6.63 |
| 2,2′,4,4′,5,5′-Hexachlorobiphenyl (PCB-153) | | $C_{12}H_4Cl_6$ | 360.88 | 6.83 |
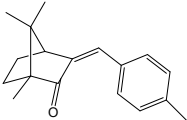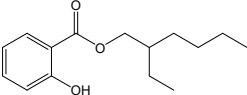
[a] $logK_{ow}$, octanol-water partition coefficients.

**Table S3** The chemical structures and properties of five PAEs.

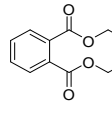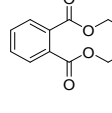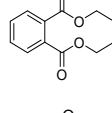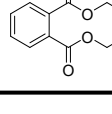| Compounds | Structures | Molecular formula | Relative molecular mass (g·mol⁻¹) | logK_ow^a |
|---|---|---|---|---|
| Dimethyl phthalate (DMP) | | $C_{10}H_{10}O_4$ | 194.19 | 1.61 |
| Diethyl phthalate (DEP) | | $C_{12}H_{14}O_4$ | 222.24 | 2.38 |
| Di-n-butyl-phthalate (DBP) | | $C_{16}H_{22}O_4$ | 278.35 | 4.45 |
| Di-n-octyl phthalate (DOP) | | $C_{24}H_{38}O_4$ | 390.56 | 8.06 |
| Di-(2-ethylhexyl) phthalate (DEHP) | | $C_{24}H_{38}O_4$ | 390.56 | 7.50 |

[a] $logK_{ow}$, octanol-water partition coefficients.

**Table S4** The chemical structures and properties of five UVFs.

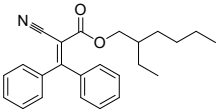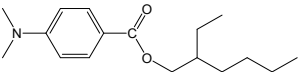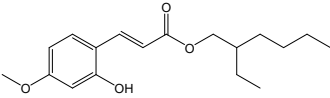| Compounds | Structures | Molecular formula | Relative molecular mass (g·mol$^{-1}$) | log$K_{ow}$[a] |
|---|---|---|---|---|
| 4-Methylbenzylidene camphor (MBC) | | $C_{10}H_{16}O$ | 152.23 | 5.47 |
| Octocrylene (OC) | | $C_{24}H_{27}NO_2$ | 361.48 | 5.97 |
| 2-Ethylhexyl 4-(dimethylamino) benzoate (OD-PABA) | | $C_{17}H_{27}NO_2$ | 277.40 | 6.15 |
| 2-Ethylhexyl 4-methoxycinnamate (EHMC) | | $C_{18}H_{26}O_3$ | 290.40 | 5.80 |
| 2-Ethylhexyl salicylate (EHS) | | $C_{15}H_{22}O_3$ | 250.33 | 5.97 |

[a] log$K_{ow}$, octanol-water partition coefficients.

## 3 Results and discussion

### 3.1 Surface pretreatment of NiTi wire
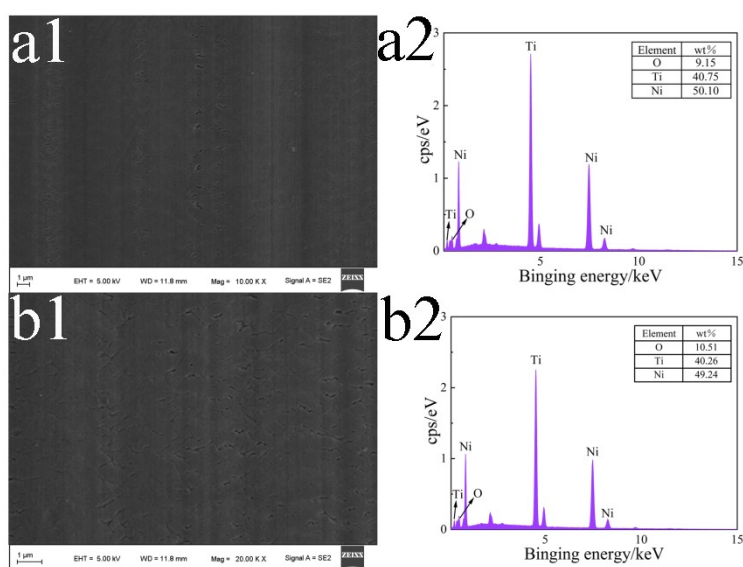


**Fig. S1** SEM images of the as-received NiTi wire (a), the NiTi wire pretreated by $HNO_3$ (b) and corresponding EDS spectra.
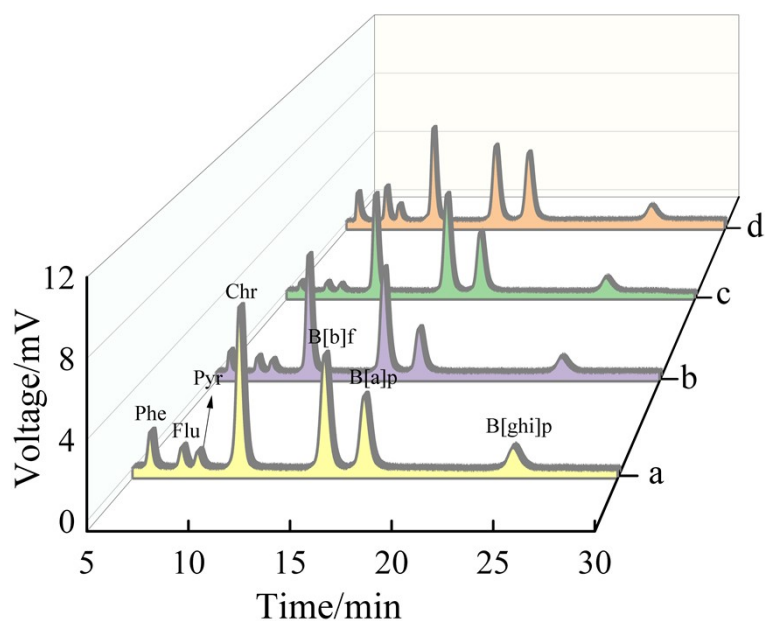
**Fig. S2** Typical chromatograms of DI-SPME-HPLC-UV with the ZnONSs coatings grown in the presence of 0.075 mol·L$^{-1}$ ZnCl$_2$ (a), 0.075 mol·L$^{-1}$ Zn(Ac)$_2$ (b), 0.075 mol·L$^{-1}$ Zn(NO$_3$)$_2$ (c) and 0.01 mol·L$^{-1}$ ZnSO$_4$ (d) for PAHs at the spiking level of 50 μg·L$^{-1}$ each analyte. Conditions: Temperature, 30 °C; Stirring rate, 400 r·min$^{-1}$; Adsorption time, 30 min; Desorption time, 4 min; NaCl, 25%(w/v); pH, 9.0.



**Fig. S3** Adsorption efficiency of the ZnONSs coatings grown in the electrolytic solutions without KCl (a) and with KCl (b) of 0.1 mol·L$^{-1}$ for PAHs at the spiking level of 50 μg·L$^{-1}$ each analyte. Conditions: Temperature, 30 °C; Stirring rate, 400 r·min$^{-1}$; Adsorption time, 30 min; Desorption time, 4 min; NaCl, 25%(w/v); pH, 9.0.
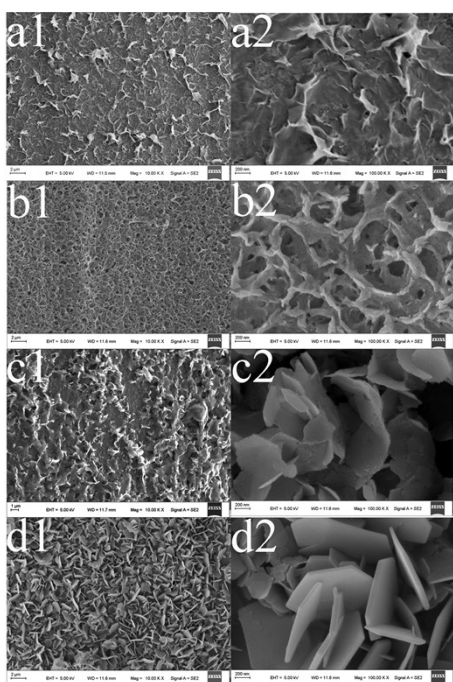
**Fig. S4** Low- (×10000) and high-magnification (×100000) SEM images of the ZnO coatings grown in the electrolytic solutions with KCl of 0.1 mol·L$^{-1}$ as well as ZnCl$_2$ of 0.01 mol·L$^{-1}$ (a1, a2), 0.025 mol·L$^{-1}$ (b1, b2), 0.05 mol·L$^{-1}$ (c1, c2) and 0.075 mol·L$^{-1}$ (d1, d2). Conditions: Applied voltage, -1.1 V; Temperature, 25 °C; Deposition time, 20 min; KCl, 0.1 mol·L$^{-1}$.
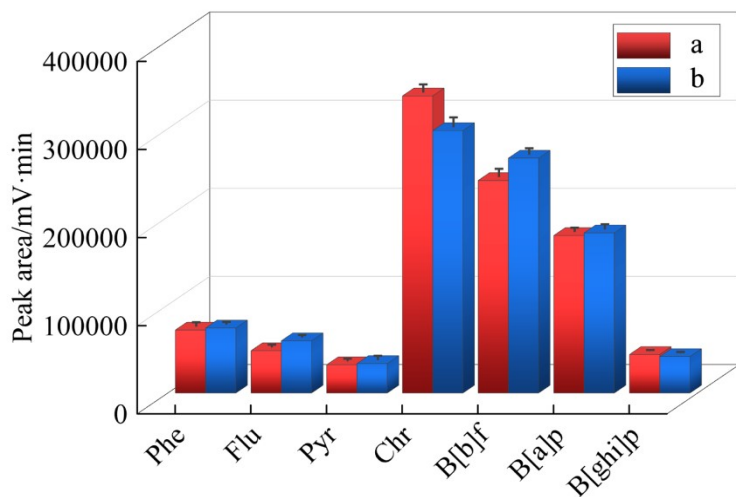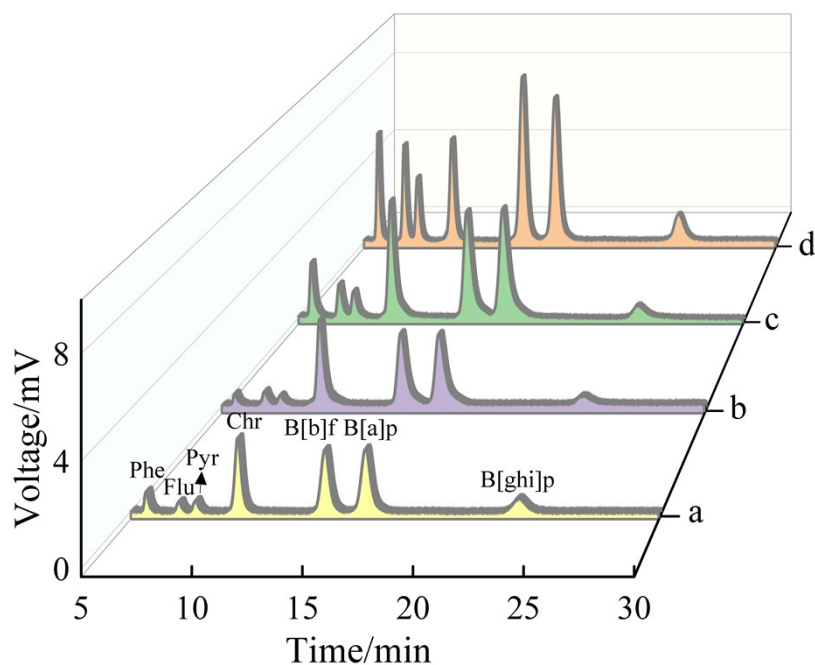


**Fig. S5** Typical chromatograms of DI-SPME-HPLC-UV with the ZnONSs coatings grown in the electrolytic solutions with KCl of 0.1 mol·L$^{-1}$ as well as ZnCl$_2$ of 0.01 mol·L$^{-1}$ (a), 0.025 mol·L$^{-1}$ (b), 0.05 mol·L$^{-1}$ (c) and 0.075 mol·L$^{-1}$ (d) at the spiking level of 50 μg·L$^{-1}$ each analyte. Conditions: Temperature, 30 °C; Stirring rate, 400 r·min$^{-1}$; Adsorption time, 30 min; Desorption time, 4 min; NaCl, 25%(w/v); pH, 9.0.
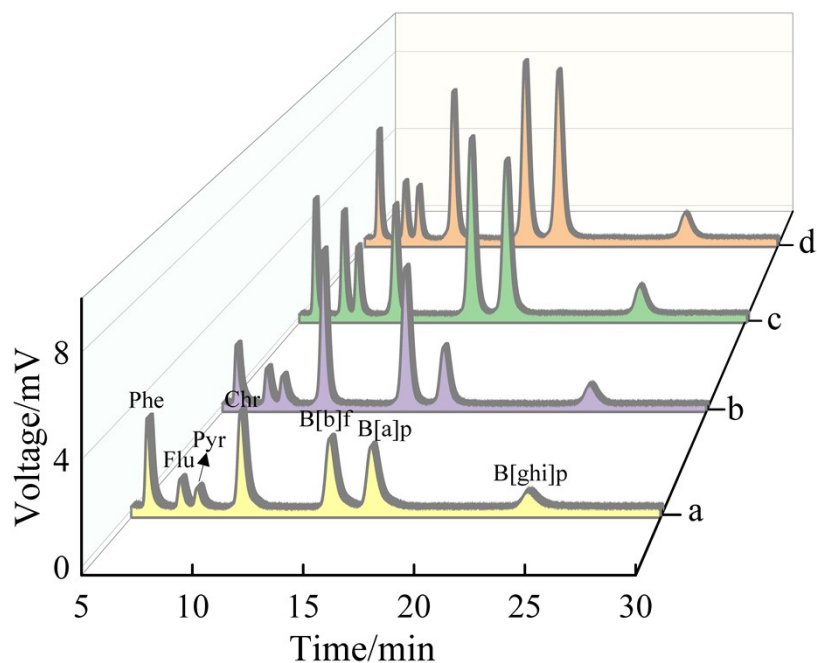
**Fig. S6** Typical chromatograms of DI-SPME-HPLC-UV with the ZnONSs coatings grown at applied voltages of -0.9 V (a), -1.0 V (b), -1.1 V (c) and -1.2 V (d) at the spiking level of 50 μg·L$^{-1}$ each analyte. Conditions: Temperature, 30 °C; Stirring rate, 400 r·min$^{-1}$; Adsorption time, 30 min; Desorption time, 4 min; NaCl, 25%(w/v); pH, 9.0.
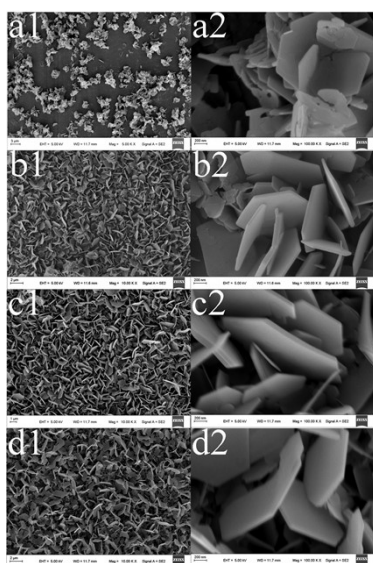


**Fig. S7** Low- (×10000) and high-magnification (×100000) SEM images of the ZnONSs coatings grown on the pretreated NiTi fibers within 10 min (a1, a2), 20 min (b1, b2), 30 min (c1, c2) and 40 min (d1, d2). Conditions: Applied voltage, -1.1 V; Temperature, 25 °C; KCl, 0.1 mol·L$^{-1}$; ZnCl$_2$, 0.075 mol·L$^{-1}$.
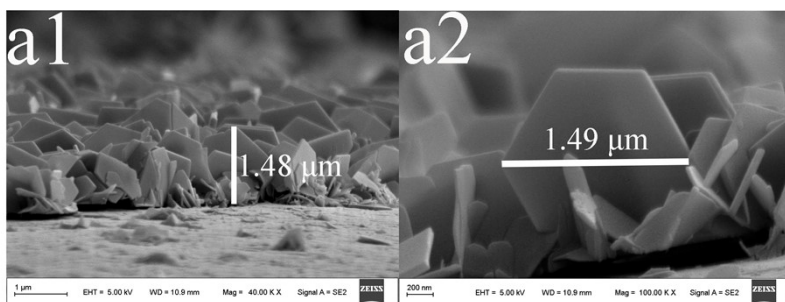
**Fig. S8** Cross-sectional views of vertically oriented hexagonal ZnONSs coatings grown in the electrolyte of 0.075 mol·L$^{-1}$ ZnCl$_2$ and 0.1 mol·L$^{-1}$ KCl at -1.1 V within 30 min.
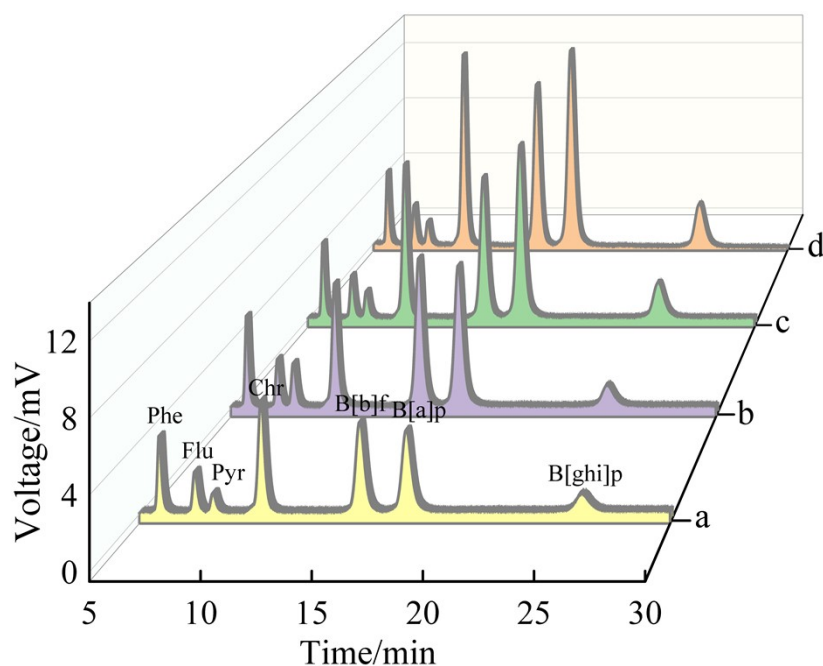


**Fig. S9** Typical chromatograms of DI-SPME-HPLC-UV with the ZnONSs coatings grown within 10 min (a), 20 min (b), 30 min (c), 40 min (d) at the spiking level of 50 μg·L$^{-1}$ each analyte. Conditions: Temperature, 30 °C; Stirring rate, 400 r·min$^{-1}$; Adsorption time, 30 min; Desorption time, 4 min; NaCl, 25%(w/v); pH, 9.0.
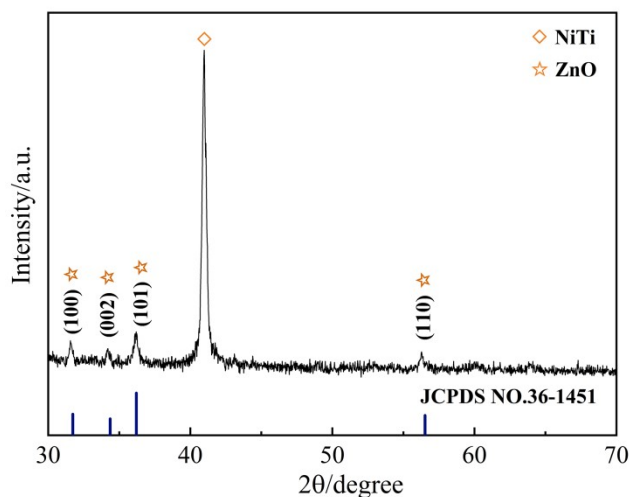
**Fig. S10** XRD pattern of the NiTi@P-ZnONSs fiber.

3.6 Optimisation of SPME conditions

In this study, the solution pH can affect the surface charge of metal oxides and extreme pH can cause damage to the P-ZnONSs coating although pH has a minor effect on the adsorption efficiency of PAHs. Thus the effect of solution pH on adsorption was investigated in the pH range of 7.0-9.5. As can be seen from Fig. S11a, the best adsorption efficiency for PAHs was achieved at pH = 9.0. Furthermore, the ionic strength of the solution was adjusted by adding NaCl of 5.0%-30%(w/v). According to Fig. S11b, the adsorption efficiency of PAHs increased with increasing concentration of NaCl. However, excessive salt concentration increased the solution viscosity, leading to an decrease in adsorption efficiency. NaCl of 25%(w/v) was used in SPME.

Stirring can improve the mass transfer of the analytes from the bulk solution to the fiber coating and reduce equilibration time. As shown in Fig. S11c, the maximum adsorption efficiency was attained at the stirring rate of 500 r·min$^{-1}$. On the contrary, vigorous stirring resulted in lower adsorption efficiency. Furthermore, adsorption temperature is a critical parameter affecting the thermodynamic and kinetic processes. Increasing the adsorption temperature is beneficial to improve the diffusion of the analyte molecules. Since adsorption is generally an exothermic process and the solubility of the analytes in water increases at elevated temperature, adsorption temperature has positive and negative effects on the adsorption efficiency of the analytes. From the results shown in Fig. S11d, 35 °C was employed in the SPME process.

In addition, sufficient adsorption time is generally required to reach adsorption equilibrium of the analytes between the fiber coating and the sample solution. Similarly some time is also needed for the desorption of the analytes in the mobile phase. As demonstrated in Fig. S11e and S11f, 50 min and 5 min were needed for adsorption and desorption, respectively.
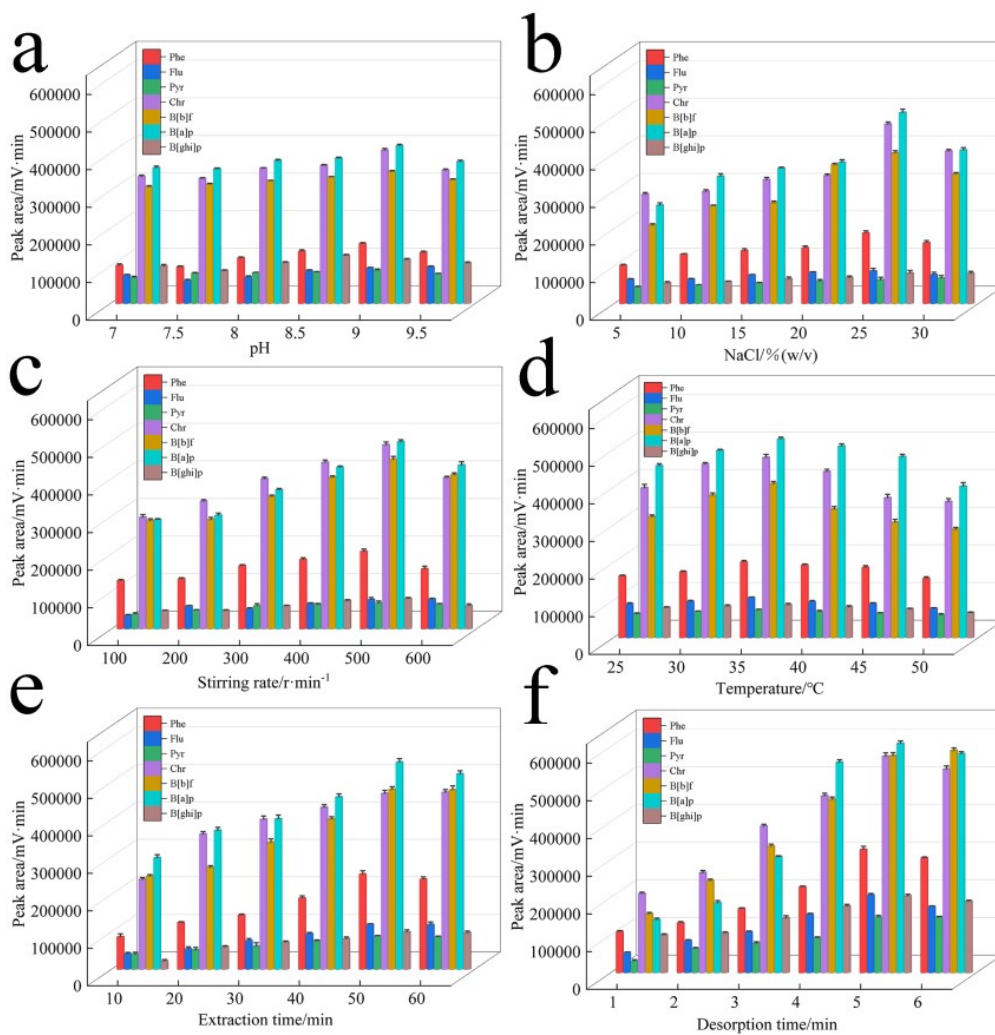
**Fig. S11** Effect of pH (a), ionic strength (b), stirring rate (c), temperature (d), adsorption time (e) and desorption time (f) on the adsorption efficiency.
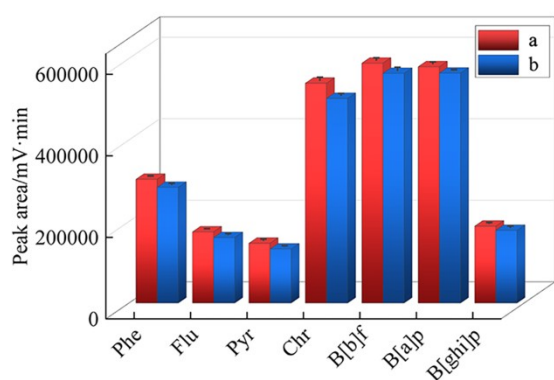


**Fig. S12** Adsorption efficiency of the NiTi@P-ZnONSs fiber for PAHs before (a) and after (b) immersing in methanol for 72 h.

**Table S5** Analytical results of PAHs in real water samples (n=3)

| Samples | Analytes | Original (μg·L⁻¹) | Spiked with 2.5 μg·L⁻¹ | | | Spiked with 10 μg·L⁻¹ | | |
|---|---|---|---|---|---|---|---|---|
| | | | Detected (μg·L⁻¹) | Recovery (%) | RSDs (%) | Detected (μg·L⁻¹) | Recovery (%) | RSDs (%) |
| River water under Xisha Bridge | Phe | ND[a] | 2.32 | 92.8 | 5.37 | 10.1 | 101. | 5.11 |
| | Flu | ND | 2.18 | 87.2 | 3.99 | 9.84 | 98.4 | 4.96 |
| | Pyr | ND | 2.34 | 93.6 | 3.71 | 9.54 | 95.4 | 5.69 |
| | Chr | ND | 2.40 | 96.0 | 4.68 | 9.97 | 99.7 | 6.01 |
| | B[b]f | ND | 2.61 | 104 | 6.91 | 9.78 | 97.8 | 7.61 |
| | B[a]p | ND | 2.35 | 94.0 | 5.98 | 10.5 | 105. | 6.98 |
| | B[ghi]p | ND | 2.31 | 92.4 | 3.64 | 8.96 | 89.6 | 5.86 |
| River water under Yintan Bridge | Phe | ND | 2.38 | 95.2 | 5.62 | 9.72 | 97.2 | 3.34 |
| | Flu | ND | 2.35 | 94.0 | 7.35 | 9.90 | 99.0 | 6.81 |
| | Pyr | ND | 2.29 | 91.6 | 3.65 | 9.86 | 98.6 | 6.68 |
| | Chr | 1.02 | 3.32 | 94.3 | 6.47 | 9.89 | 89.7 | 5.08 |
| | B[b]f | ND | 2.19 | 87.6 | 3.79 | 10.0 | 100 | 6.99 |
| | B[a]p | 0.55 | 2.97 | 97.4 | 3.76 | 9.99 | 99.9 | 7.63 |
| | B[ghi]p | ND | 2.41 | 96.4 | 7.31 | 9.92 | 99.2 | 6.41 |
| Wastewater | Phe | ND | 2.42 | 97.3 | 3.75 | 9.39 | 94.1 | 7.31 |
| | Flu | ND | 2.07 | 82.8 | 4.90 | 9.33 | 93.3 | 5.30 |
| | Pyr | ND | 2.40 | 96.0 | 4.38 | 9.84 | 98.4 | 7.83 |
| | Chr | 0.78 | 3.15 | 96.0 | 5.14 | 10.8 | 101 | 4.96 |
| | B[b]f | 0.96 | 3.49 | 101 | 5.66 | 10.9 | 99.2 | 5.28 |
| | B[a]p | 1.32 | 3.76 | 98.4 | 5.94 | 11.6 | 103 | 8.58 |
| | B[ghi]p | ND | 2.44 | 97.6 | 3.47 | 9.88 | 98.8 | 5.41 |
| Lake water | Phe | ND | 2.38 | 95.2 | 7.02 | 9.98 | 99.8 | 5.19 |
| | Flu | ND | 2.27 | 90.8 | 7.75 | 10.1 | 101 | 7.54 |
| | Pyr | ND | 2.32 | 92.8 | 6.14 | 9.77 | 97.7 | 6.01 |
| | Chr | ND | 2.52 | 101 | 5.14 | 9.89 | 98.9 | 6.54 |
| | B[b]f | ND | 2.38 | 95.2 | 4.19 | 10.0 | 100 | 4.72 |
| | B[a]p | ND | 2.44 | 97.6 | 5.68 | 9.81 | 98.1 | 3.80 |
| | B[ghi]p | ND | 2.29 | 91.6 | 5.13 | 9.76 | 97.6 | 5.38 |
| Rain water | Phe | ND | 2.43 | 97.2 | 7.35 | 9.69 | 96.9 | 7.75 |
| | Flu | 0.43 | 2.94 | 100 | 5.04 | 10.0 | 96.3 | 6.60 |
| | Pyr | ND | 2.28 | 91.2 | 6.44 | 9.34 | 93.4 | 5.45 |
| | Chr | ND | 2.26 | 90.4 | 7.46 | 9.76 | 97.6 | 4.67 |
| | B[b]f | ND | 2.43 | 97.2 | 5.80 | 10.2 | 102 | 4.68 |
| | B[a]p | 0.86 | 3.27 | 97.3 | 3.78 | 10.5 | 96.2 | 6.85 |
| | B[ghi]p | ND | 2.45 | 98.0 | 4.67 | 9,62 | 96.2 | 4.33 |

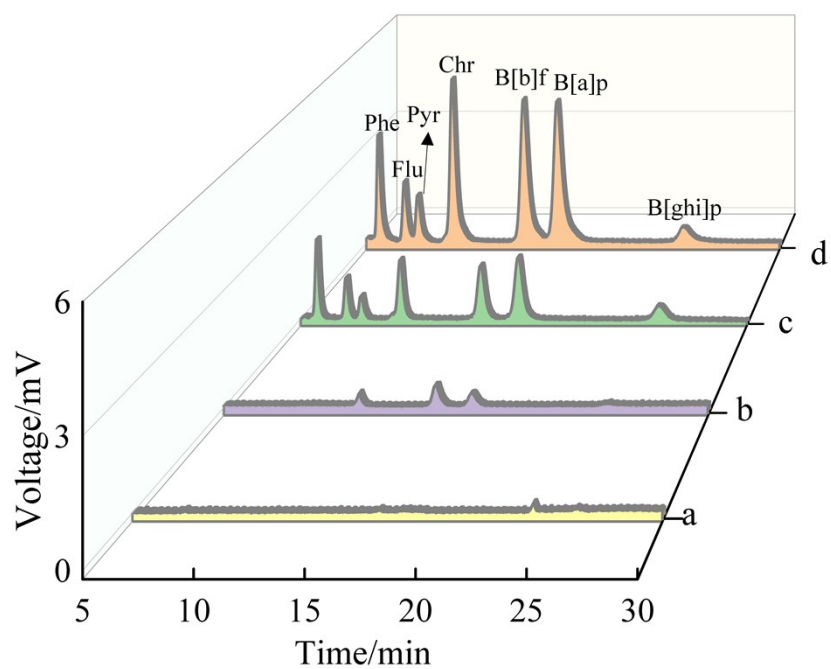[a] ND, Not detected or lower than LODs

**Fig. S13** Typical chromatograms of direct HPLC (a) and DI-SPME-HPLC-UV with the NiTi@P-ZnONSs fiber for target PAHs in wastewater (b), and wastewater spiked with 2.5 $\mu g \cdot L^{-1}$ (c) and 10 $\mu g \cdot L^{-1}$ (d).